see commentary on page 8

Distinct roles of Mac-1 and its counter-receptors in neonatal obstructive nephropathy

B Lange-Sperandio[1], K Schimpgen[1], B Rodenbeck[1], T Chavakis[2,3], A Bierhaus[2], P Nawroth[2], B Thornhill[4], F Schaefer[1] and RL Chevalier[4]

[1]Department of Pediatrics, University of Heidelberg, Heidelberg, Germany; [2]Department of Internal Medicine I, University of Heidelberg, Heidelberg, Germany; [3]Experimental Immunology Branch, NCI, National Institutes of Health, Bethesda, Maryland, USA and [4]Department of Pediatrics, University of Virginia, Charlottesville, Virginia, USA

Urinary tract obstruction during renal development leads to tubular atrophy and interstitial fibrosis. Inflammatory macrophages are crucial in this process, and β_2-integrins play a major role in leukocyte recruitment. We investigated the role of β_2-integrins and their major counter-receptors (intercellular adhesion molecule-1 (ICAM-1), receptor for advanced glycation endproducts (RAGE), junctional adhesion molecule (JAM)-C) in obstructive nephropathy in neonatal mice. Two-day-old β_2-integrin-deficient mice (Mac-1$^{-/-}$ and LFA-1$^{-/-}$(deficient for leukocyte function-associated antigen-1)) and wild-type mice (C57BL/6) underwent unilateral ureteral obstruction (UUO) or sham operation. After 1, 5 or 12 days of obstruction, renal macrophage infiltration and tubulointerstitial damage were quantitated. Tissue abundance of Mac-1 and its ligands ICAM-1, RAGE and JAM-C was examined by Western blot and immunoprecipitation. Deficiency of either integrin was associated with reduced early macrophage invasion into the obstructed kidney. After 12 days of UUO, macrophage infiltration and tubulointerstitial injury were reduced only in Mac-1$^{-/-}$ but not in LFA-1$^{-/-}$ mice. Besides ICAM-1, an upregulation of two novel Mac-1 ligands, RAGE and JAM-C were observed, however, with distinct time courses. We conclude that β_2-integrins mediate macrophage infiltration in UUO. Mac-1 is the predominant leukocyte integrin involved in leukocyte recruitment after obstruction. ICAM-1 and its new ligands RAGE and JAM-C are sequentially activated in UUO. Blocking of Mac-1 and its ligands may confer synergistic renoprotective effects in neonatal obstructive nephropathy.

Kidney International (2006) **69,** 81–88. doi:10.1038/sj.ki.5000017

KEYWORDS: integrins; Mac-1; unilateral ureteral obstruction; macrophages; RAGE; JAM

Correspondence: *B Lange-Sperandio, Department of Pediatrics, University of Heidelberg, INF 150, 69120 Heidelberg, Germany. E-mail: baerbel.lange-sperandio@med.uni-heidelberg.de*

Received 25 May 2005; revised 7 July 2005; accepted 22 July 2005

Congenital obstructive nephropathy is a major cause of kidney failure in infants and children.[1] Chronic unilateral ureteral obstruction (UUO) leads to interstitial inflammation, interstitial fibrosis and tubular atrophy.[2,3] Central to these events is the acute macrophage infiltration of the tubulointerstitium, which is preceded by local upregulation of macrophage chemokines and adhesion molecules.[4–11] Macrophages contribute to the tubulointerstitial injury by releasing proinflammatory cytokines and cytotoxic substances,[12,13] by inducing apoptosis in tubular cells[14] and by activating interstitial fibroblasts.[15,16] Although the selective infiltration of the interstitium by macrophages in UUO is well established,[17,18] the molecular mechanisms underlying the recruitment of these immune cells in UUO are poorly defined. In particular, although the expression of β_2-integrins and their major endothelial ligand intercellular adhesion molecule-1 (ICAM-1) has been investigated in UUO,[19,20] there are no comprehensive studies assessing the functional role of these molecules in the pathogenesis of UUO.

The recruitment of leukocytes from the circulation and their subsequent influx into surrounding tissues at sites of inflammation or injury requires multistep adhesive and signalling events, including selectin-mediated capture and rolling, leukocyte activation, integrin-mediated firm adhesion and their subsequent transendothelial migration.[21] During firm adhesion of leukocytes to the endothelium, members of the β_2-integrin family, leukocyte function-associated antigen-1 (LFA-1) ($\alpha L\beta_2$, CD11a/CD18) and Mac-1 ($\alpha M\beta_2$, CD11b/CD18) on the leukocyte surface, interact with endothelial counter-receptors such as ICAM-1 and surface-associated fibrinogen. LFA-1 and Mac-1 are exclusively expressed on leukocytes. Whereas LFA-1 contributes to leukocyte rolling by stabilizing the transient attachment, Mac-1 contributes to emigration from the vessel, suggesting that LFA-1 and Mac-1 serve sequential rather than parallel functions.[22,23] In UUO, expression of ICAM-1 has been shown by immunohistochemistry on tubular epithelial cells, interstitial cells and endothelial cells.[24] However, in ICAM-1 antisense oligonucleotide-treated mice, macrophage infiltration following UUO was reduced but not eliminated, suggesting that additional β_2-integrin counter-receptors may

be operative in leukocyte recruitment.[25] Recently, receptor for advanced glycation endproducts (RAGE), a multiligand receptor on vascular cells centrally involved in inflammatory processes,[26] was identified as a new β_2-integrin counterligand. RAGE binds to Mac-1 but not to LFA-1.[27] RAGE is expressed at low levels in normal tissues but becomes upregulated at inflammatory sites where its ligands accumulate.[28–30] Other ligands for the β_2-integrins include the family of junctional adhesion molecules (JAMs). JAMs are a family of three glycoproteins (JAM-A, -B, -C) participating in junction assembly, platelet activation and leukocyte transmigration.[31–33] JAMs localize to intercellular junctions of polarized endothelial and epithelial cells, but are also expressed on leukocytes and platelets. JAM-C is expressed in vascular endothelial cells, including high endothelial venules, in epithelial cells and platelets.[34] JAM-C binds to Mac-1 but not to LFA-1 and has a direct role in leukocyte transmigration.[35,36]

Because most glomeruli continue to form postnatally in mice, renal development in the neonatal mouse is analogous to renal development in the human fetus. For this reason, surgical ligation of one ureter in newborn mice is a model to study the effects of urinary tract obstruction on renal development. The present study was designed to characterize the role of the β_2-integrins and their ligands (ICAM-1, RAGE, JAM-C) in UUO in newborn mice.

RESULTS

Normal kidney morphology in LFA-1$^{-/-}$ and Mac-1$^{-/-}$ mice

LFA-1$^{-/-}$ and Mac-1$^{-/-}$ mice appeared healthy and developed without apparent defects. The kidneys from the LFA-1$^{-/-}$ and Mac-1$^{-/-}$ mutants grossly presented similar to those from wild-type (WT) mice. Light microscopic examinations of the kidney showed normal structure of the kidney, that is, glomeruli, tubulointerstitium and blood vessels (not shown). Obstructed kidneys of LFA-1$^{-/-}$, Mac-1$^{-/-}$ and WT mice presented with hydronephrosis at 1, 5 and 12 days after obstruction. The degree of tubulointerstitial injury was dependent on the β_2-integrin deficiency and the duration of obstruction. Whereas macrophage infiltration and tubular apoptosis were noted from day 1 after UUO, tubular atrophy and interstitial fibrosis were present from day 5 onwards.

Monocyte/macrophage recruitment

UUO resulted in a significant and progressive increase in interstitial macrophage infiltration in all obstructed WT, LFA-1$^{-/-}$ and Mac-1$^{-/-}$ kidneys when compared to sham-operated controls and unobstructed intact opposite kidneys (Figure 1a–c, 2a and b). β_2-Integrin-deficient mice showed a significant decrease in interstitial macrophage infiltration into the obstructed kidney when compared to WT; both Mac-1$^{-/-}$ and LFA-1$^{-/-}$ demonstrated a decrease by 97% at day 1 after UUO (WT 112.7 ± 20, LFA-1$^{-/-}$ 3.0 ± 0.9, Mac-1$^{-/-}$ 2.7 ± 0.7; $P < 0.001$). At 5 days after obstruction, Mac-1$^{-/-}$ demonstrated a decrease by 88% ($P < 0.001$) and LFA-1$^{-/-}$ showed a decrease by 74% ($P < 0.001$) when compared to WT (Figure 2a). Mac-1$^{-/-}$ still showed a significant reduction in macrophage infiltration at 12 days after UUO (decrease by 78%, $P < 0.05$) (Figure 1c).

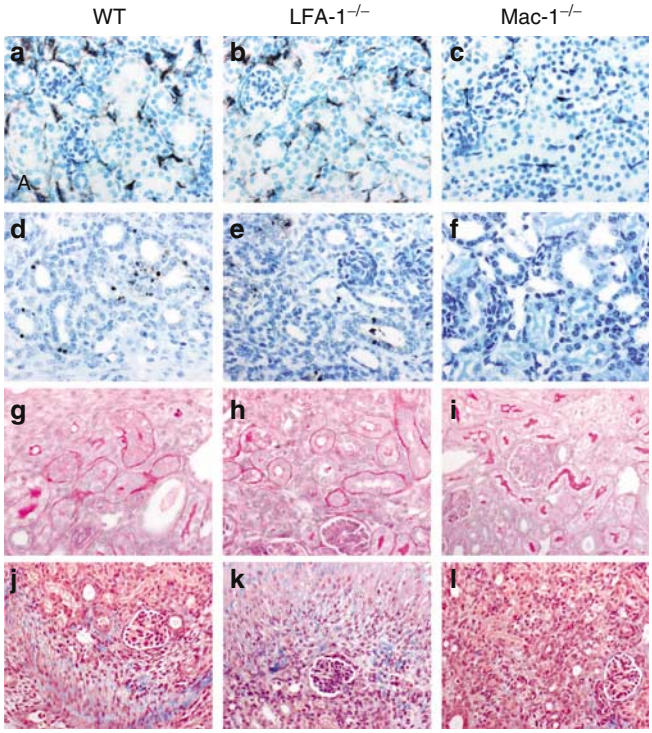

Figure 1 | Representative photomicrographs of obstructed kidneys (UUO). Renal sections were stained for macrophage infiltration (F4/80 antibody) at 12 days after UUO in control mice (**a**), β_2-integrin-deficient LFA-1$^{-/-}$ mice (**b**) and Mac-1$^{-/-}$ mice (**c**); original magnification $\times 400$. Mac-1$^{-/-}$ kidneys showed significantly fewer macrophages (black). Tubular apoptosis (TUNEL) at 12 days after obstruction in control mice (**d**), LFA-1$^{-/-}$ mice (**e**) and Mac-1$^{-/-}$ mice (**f**); original magnification $\times 400$. Mac-1$^{-/-}$ kidneys showed fewer TUNEL-positive tubular cells. Periodic acid Schiff staining identified the thickened, irregular tubular basement membrane characteristic of tubular atrophy in: control mice (**g**), LFA-1$^{-/-}$ mice (**h**) and Mac-1$^{-/-}$ mice (**i**) at day 12 after UUO. Renal sections were stained with Masson's trichrome to detect interstitial collagen (blue) in: WT mice (**j**), LFA-1$^{-/-}$ mice (**k**) and Mac-1$^{-/-}$ mice (**l**) at day 12 following UUO; original magnification $\times 250$.

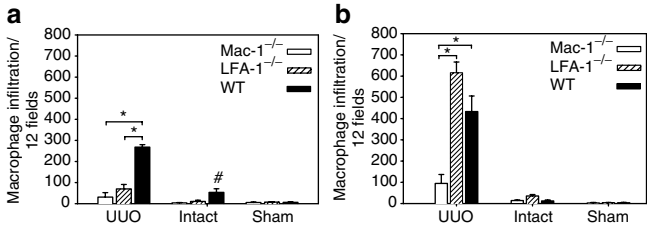

Figure 2 | Relative area of macrophage infiltration, identified by F4/80 antibody (a) 5 days and (b) 12 days after operation in Mac-1$^{-/-}$, LFA-1$^{-/-}$ and WT mice. Twelve fields were analyzed at a magnification of $\times 400$. Intact = intact opposite kidney, UUO = obstructed kidney, Sham = sham-operated control. $^{*}P < 0.05$. $^{\#}P < 0.05$ versus sham-operated control.

Notably, macrophage infiltration in LFA-$1^{-/-}$ mice was not different from that of WT at 12 days after obstruction (Figure 2b). An increase in interstitial macrophage infiltration was also noted in the contralateral (intact opposite) kidneys in either Mac-$1^{-/-}$ or LFA-$1^{-/-}$ or WT mice with UUO.

Tubular apoptosis

Tubular apoptosis was significantly increased in all obstructed kidneys when compared to intact opposite kidneys at days 1, 5 and 12 after UUO (Figures 3a and b). Interestingly, only Mac-$1^{-/-}$ mice showed a significant decrease in tubular apoptosis when compared to WT at all time points measured. Tubular apoptosis in the obstructed kidney decreased by 62% in Mac-$1^{-/-}$ at day 1, by 51% at day 5 and by 35% at day 12 after UUO, when compared to both WT and LFA-$1^{-/-}$ ($P<0.05$) (Figures 1d–f). LFA-$1^{-/-}$ mice showed a decrease in tubular apoptosis by 22% at day 5, which was not significant. At day 12 after UUO, tubular apoptosis in the obstructed kidney of LFA-$1^{-/-}$ mice was not different from that of WT but significantly higher than that in Mac-$1^{-/-}$ ($P<0.05$) (Figure 3b).

Tubular atrophy

Tubular atrophy in the obstructed kidney was detectable as early as 5 days after UUO (Figure 4a). At 12 days after UUO, there was a dramatic increase in thickened and sometimes duplicated tubular basement membranes in WT mice (Figure 1g–i and 4b). By contrast, tubular atrophy in Mac-$1^{-/-}$ mice was lower by 48% at day 5, and by 41% at day 12 after UUO, compared to both WT and LFA-$1^{-/-}$ ($P<0.05$). The number of atrophic tubules was not different in LFA-$1^{-/-}$ mice compared to that in WT. Intact opposite kidneys and sham-operated controls had no signs of tubular atrophy.

Interstitial fibrosis

Collagen deposition was clearly stained and confined to the renal interstitium. In obstructed kidneys of WT, Mac-$1^{-/-}$ and LFA-$1^{-/-}$ mice at 5 and 12 days after UUO, interstitial collagen was markedly increased in the interstitial space compared with intact opposite kidneys and sham-operated controls (Figure 5a and b). The deposition of interstitial collagen in UUO was significantly less pronounced in Mac-$1^{-/-}$ mice than in WT or LFA-$1^{-/-}$ mice at 12 days after UUO (Figure 1j–l). Mac-$1^{-/-}$ showed a decrease in interstitial fibrosis by 25% at day 5 after UUO, and by 32% at day 12 after UUO, when compared to WT ($P<0.05$). At day 1 after obstruction, as well as in intact opposite controls and sham-operated kidneys, there was no interstitial collagen deposition in β_2-integrin-deficient and WT mice at all time points studied.

Expression of Mac-1 ligands in UUO

ICAM-1 protein was present in obstructed and non-obstructed kidneys, being highest 24 h after obstruction, followed by a gradual downregulation to day 12 after obstruction in UUO kidneys (Figure 6). ICAM-1 abundance normalized to β-actin was significantly higher in obstructed kidneys than in sham-operated controls. RAGE protein (42–46 kDa) is constitutively expressed in the skin and the lung, but inducible in other organs such as the kidney. Lung tissue was used as a positive control. RAGE was present in obstructed and non-obstructed kidneys, being highest 24 h after obstruction, followed by a gradual downregulation to day 12 after obstruction in UUO kidneys (Figure 6). RAGE abundance was significantly increased in UUO tissue lysates immunoprecipitated with Mac-1, but not in LFA-1 immunoprecipitates, indicative of the colocalization of Mac-1 and RAGE on infiltrating macrophages in the kidney (Figure 7).

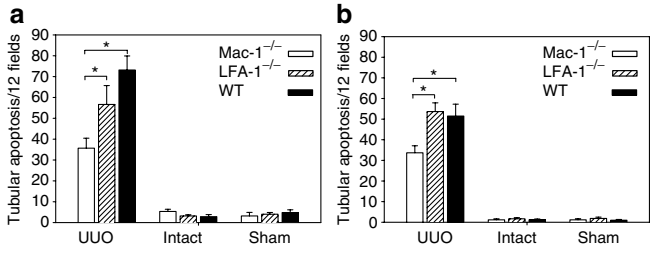

Figure 3 | Density of apoptotic tubular cells, identified by TUNEL technique (a) 5 days and (b) 12 days after operation in Mac-$1^{-/-}$, LFA-$1^{-/-}$ and WT mice. Twelve fields were analyzed at a magnification of $\times$ 400. Intact = intact opposite kidney, UUO = obstructed kidney, Sham = sham-operated control. *$P<0.05$.

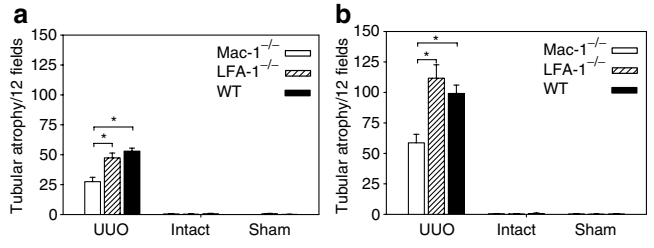

Figure 4 | Density of atrophic tubules, identified by periodic acid Schiff staining (a) 5 days and (b) 12 days after operation in Mac-$1^{-/-}$, LFA-$1^{-/-}$ and WT mice. Twelve fields were analyzed at a magnification of $\times$ 400. Intact = intact opposite kidney, UUO = obstructed kidney, Sham = sham-operated control. *$P<0.05$.

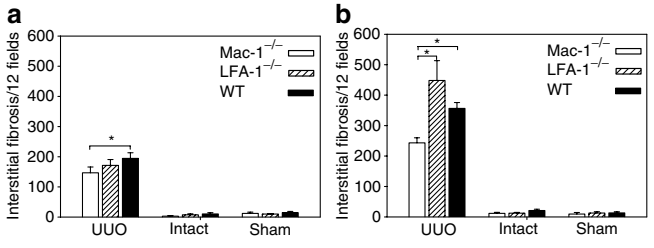

Figure 5 | Relative area of interstitial collagen, identified by Masson trichrome staining, (a) 5 days and (b) 12 days after operation in Mac-$1^{-/-}$, LFA-$1^{-/-}$ and WT mice. Twelve fields were analyzed at a magnification of $\times$ 400. Intact = intact opposite kidney, UUO = obstructed kidney, Sham = sham-operated control. *$P<0.05$.

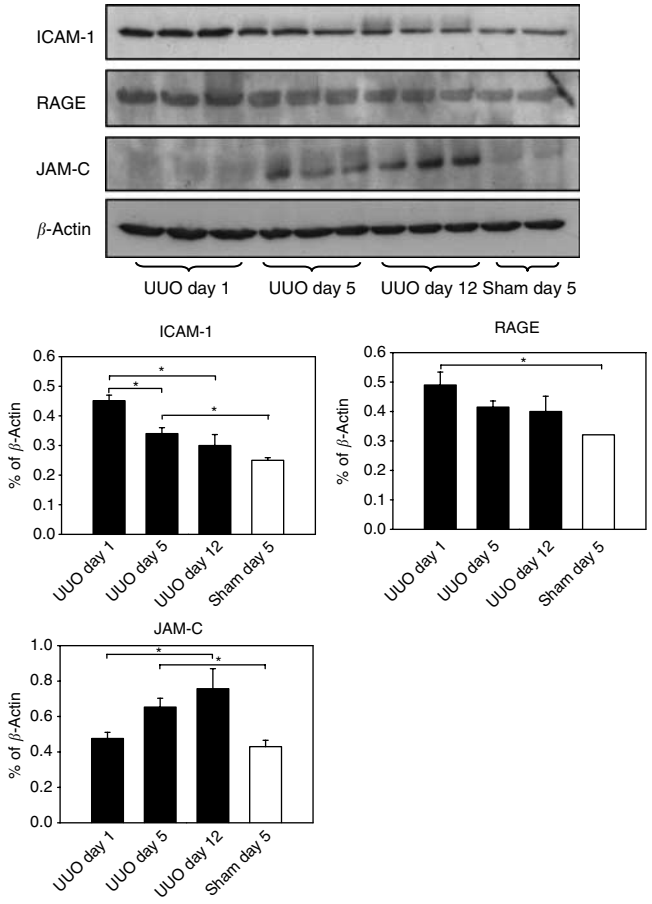

Figure 6 | Expression of Mac-1 ligands (ICAM-1, RAGE and JAM-C) in obstructed WT kidneys at 1, 5 and 12 days after obstruction and in sham-operated controls at 5 days after surgery by Western blot analysis. In UUO kidneys, ICAM-1 and RAGE (42–45 kDa) expression peaked early at 24 h after obstruction and were downregulated over time. JAM-C (42 kDa) expression increased by day 5 and peaked late at day 12 after UUO, serving as ligand for Mac-1 but not for LFA-1. β-Actin (42 kDa) demonstrated equal loading (shown for JAM-C). $^*P < 0.05$.

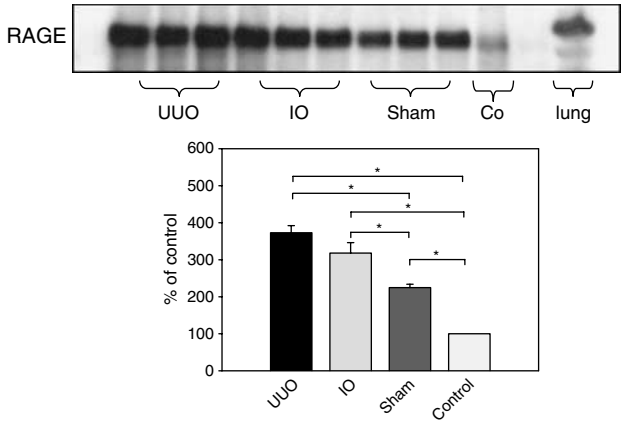

Figure 7 | Western blot for RAGE on Mac-1 immunoprecipitated membrane. After immunoprecipitation for Mac-1, RAGE was significantly upregulated in UUO kidneys at day 5 after obstruction, suggesting colocalization of Mac-1 and RAGE on macrophages. Kidney samples from day 5 after UUO without immunoprecipitation for Mac-1 served as control. Lung tissue was used as a positive control for RAGE. UUO = obstructed kidney, IO = intact opposite (contralateral) kidney, sham = sham-operated control kidney. $^*P < 0.05$.

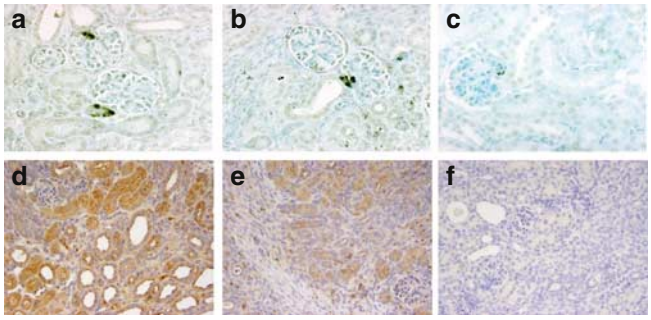

Figure 8 | Representative photomicrograph of JAM-C and ICAM-1 expression in obstructed and control kidneys. JAM-C localizes to the afferent and efferent arterioles of the juxtaglomerulus apparatus and is upregulated 12 days following UUO (**a** and **b**). Some tubular structures of the macula densa seem to be JAM-C positive as well (**a**). Sham-operated control kidneys show reduced JAM-C expression (**c**). Original magnification of $\times 400$. ICAM-1 localizes to the tubular cells and tubulointerstitial space at (**d**) 1 day and (**e**) 12 days after UUO. Control section without primary ICAM-1 antibody (**f**). Original magnification $\times 250$.

The expression of JAM-C (42 kDa) exhibited a different time course with a steady increase during the first 2 weeks following UUO (Figure 6). Moreover, we studied the localization of JAM-C and ICAM-1 in obstructed and sham-operated WT kidneys. JAM-C was clearly stained and localized to the juxtaglomerular arterioles (Figure 8a and b). Following UUO, JAM-C expression was markedly increased at day 12. Some distal tubular structures (macula densa area) showed positive staining after UUO as well (Figure 8a). In contrast, sham-operated control kidneys demonstrated only weak expression of JAM-C on the endothelial cells of the vasa afferens and efferens of the glomeruli (Figure 8c). ICAM-1 expression was clearly stained and localized to the tubular cells, renal interstitium and vessels of obstructed kidneys (Figure 8d–f).

DISCUSSION

This study addresses the role of the β_2-integrins LFA-1 and Mac-1 and their ligands ICAM-1, RAGE and JAM-C in tubulointerstitial renal disease induced by UUO. We showed that β_2-integrins mediate macrophage infiltration in obstructive nephropathy in newborn mice. The absence of either Mac-1 (Mac-$1^{-/-}$ mice) or LFA-1 (LFA-$1^{-/-}$ mice) was associated with a marked reduction in macrophage infiltration into the tubulointerstitium compared to WT controls during the first week following UUO. The decrease in macrophage influx was more pronounced in Mac-$1^{-/-}$ mice than in LFA-$1^{-/-}$ mice at day 12 after obstruction, demonstrating the predominant role of Mac-1 in leukocyte recruitment following UUO. This decrease in macrophage infiltration cannot be explained by reduced leukocyte or mononuclear cell counts in Mac-1- and LFA-1-deficient

mice, because β_2-integrin-deficient mice display varying degrees of leukocytosis.[22] In addition, Mac-$1^{-/-}$ but not LFA-$1^{-/-}$ mice, were partially protected from tubulointerstitial damage after obstruction: tubular apoptosis, tubular atrophy and interstitial fibrosis were markedly reduced in Mac-$1^{-/-}$ but not in LFA-$1^{-/-}$ mice. These results strongly indicate that Mac-1 plays a dominant role in the initiation and progression of obstructive nephropathy, and that other adhesion molecules are not able to compensate for the loss of this β_2-integrin.

The mechanisms underlying the distinct phenotypes of Mac-1- and LFA-1-deficient mice in the UUO model might be several: first, the distinct expression of the β_2-integrin counter-receptors may determine the functional role of each of these two β_2-integrins. In particular, both Mac-1 and LFA-1 seem to be important for early macrophage recruitment. This period overlaps with the expression of ICAM-1, which is a ligand for both integrins. In contrast, late macrophage recruitment is only diminished in Mac-1-deficient mice. At this point, ICAM-1 is downregulated and JAM-C is upregulated, and consistent with previous reports, JAM-C acts as a ligand only for Mac-1.[34,36] This also explains why late macrophage recruitment recovers in LFA-1-deficient mice to a degree comparable to WT mice. Secondly, Mac-1 and LFA-1 have been reported to display different functions in several aspects. For example, only Mac-1, but not LFA-1, can interact with components of the fibrinolytic system, such as plasminogen and urokinase, and modulate the pericellular proteolytic activity of leukocytes in concert with the urokinase receptor.[37,38] Moreover, Mac-1 directly interacts with the urokinase receptor, whereas LFA-1 does not.[39] Accordingly, the phenotype of Mac-1-deficient mice in UUO shares some similarities with the phenotype of the urokinase receptor-deficient mice in the same model.[11]

The β_2-integrins and their ligands mediate macrophage infiltration in other models of kidney diseases. In diabetic nephropathy, the expression of the β_2-integrin ligand ICAM-1 was associated with the progression of kidney disease.[40] Mac-1 participates in leukocyte activation, recruitment and the development of immune complex glomerulonephritis in several models.[41,42] In UUO, expression of Mac-1 and its ligand ICAM-1 in the obstructed kidney has been demonstrated by immunohistochemistry.[19,25] Recently, Yamagishi *et al.*[24] could show that genetically modified cells expressing Mac-1 are capable of migration to sites of ICAM-1 expression and deliver anti-inflammatory cytokines in UUO. ICAM-1 expression has been shown in the interstitium in areas of intense macrophage infiltration, in tubular epithelial cells and vessels of the renal cortex after UUO.[20,24] Whereas ICAM-1 was expressed within 3 days after UUO induction in adult mice, peaking at day 5 and remaining high up to day 14,[24] we observed a different pattern of expression in neonatal UUO. ICAM-1 protein abundance was highest at 24 h after obstruction, followed by a gradual downregulation to day 14. In addition, we could show that the newly discovered Mac-1 counter-receptors RAGE and JAM-C are weakly expressed (RAGE) or not yet upregulated (JAM-C) at 24 h after obstruction. This demonstrates the predominant role of ICAM-1 as counter-receptor for Mac-1 and LFA-1 in early stages of neonatal UUO. Besides leukocyte recruitment and proliferation of macrophages *in situ*, different residence times within the obstructed kidney may also contribute to the net accumulation of leukocytes after UUO.

While RAGE is constitutively expressed during embryonic development, its expression is downregulated in most organs in adult life.[43] Macrophages, endothelial cells, neuronal cells and fibroblasts do not express significant amounts of RAGE under physiological conditions, but can be induced to express RAGE at inflammatory sites where its ligands accumulate.[28–30] Recently, it has been shown that RAGE functions as an endothelial adhesion receptor during inflammation that directly interacts with Mac-1, thereby mediating leukocyte recruitment.[27,44] Consistently, RAGE abundance was significantly increased in UUO tissue lysates immunoprecipitated with Mac-1, but not in LFA-1 immunoprecipitates, also suggesting the colocalization of Mac-1 and RAGE on infiltrating macrophages in the kidney.

JAM-C, another ligand for Mac-1, was highly upregulated following obstruction. JAM-C expression increased 5 days after UUO and increased further on day 12 in obstructed kidneys, showing a delayed pattern compared to ICAM-1 and RAGE. Being strategically located at the apical part of intercellular spaces, this JAM protein plays an important role in inflammation and, in particular, during the passage of leukocytes across interendothelial spaces.[45,46] Thus, in the UUO model, the binding of Mac-1 to JAM-C may facilitate leukocyte infiltration into the obstructed kidneys, guiding the various leukocyte subsets to the appropriate sites of activation and effector function. Although the expression of JAM-C on endothelial cells is consistent with its role in leukocyte recruitment, juxtaglomerular arterioles have not been shown to participate in leukocyte transmigration. We also observed some staining on non-vascular structures in the distal tubule. This suggests that JAM-C may be involved in additional functions to those associated with leukocyte extravasation, such as the tubular barrier function.

In conclusion, this study demonstrates that the β_2-integrin Mac-1 is an important mediator of macrophage infiltration in UUO, leading to tubular apoptosis, tubular atrophy and interstitial fibrosis. The expression of its ligands follows a distinct pattern and may thereby contribute to the tubulointerstitial injury. The Mac-1 interaction with JAM-C seems to be of pivotal importance. Inhibition of the β_2-integrin Mac-1 and its ligands could be an attractive approach to protect kidneys from progressive obstructive nephropathy.

MATERIALS AND METHODS

Experimental protocol

LFA-$1^{-/-}$ mice, deficient for leukocyte function-associated antigen-1 (LFA-1, $\alpha L\beta 2$, CD11a/CD18), as recently described,[47] and Mac-$1^{-/-}$ mice, deficient for the Mac-1 integrin ($\alpha M\beta 2$, CD18/CD11b)[48] were kindly provided by Dr C Ballantyne, Baylor College Houston,

Texas. Mutant mice were backcrossed into a C57BL/6 background for at least six generations and maintained in specific pathogen-free conditions. Integrin deficiency was confirmed by polymerase chain reaction. WT mice of the same genetic background (C57BL/6) were used as controls. Forty-eight hours after birth, male and female mice were subjected to complete left ureteral obstruction ($n=18$ in each group of WT, LFA-$1^{-/-}$ and Mac-$1^{-/-}$ mice) or a sham operation ($n=18$ in each group of WT, LFA-$1^{-/-}$ and Mac-$1^{-/-}$ mice) under general anesthesia with isoflurane and oxygen. With the aid of a Wild M3Z stereomicroscope (Leica, Heerbrugg, Switzerland), the distal ureter was exposed through a longitudinal 5-mm left abdominal incision and ligated twice with 6-0 silk suture. In sham-operated animals, the ureter was exposed and repositioned without further manipulation. Neonatal mice were killed at 1, 5 and 12 days after obstruction ($n=6$ in each group). The experimental protocol was approved by the Ethics Review Commitee for Animal Experimentation of the University of Virginia and the Commitee for Animal Experimentation of the University of Heidelberg.

Identification and quantitation of infiltrating monocytes/macrophages

Infiltration of monocytes/macrophages was examined by immunohistochemistry as previously described.[9] Formalin-fixed, paraffin-embedded 3 μm sections were subjected to antigen retrieval and incubated with rat anti-mouse monoclonal F4/80 antibody (supernatant from F4/80 hybridoma cells; ATCC, Manassas, VA) against monocytes/macrophages. Digital images of the sections ($n=6$ in each group) were superimposed on a grid, and the number of grid points overlapping dark brown macrophages in the cortex and medulla was recorded for each field. Twelve non-overlapping fields at $\times 400$ magnification were analyzed in a blinded fashion. Twelve fields at $\times 400$ magnification covered the whole obstructed kidney, especially in very young kidneys at day 1 after obstruction. Data were expressed as the mean score $\pm$ s.e.m. per 12 high-power fields. Representative photomicrographs of macrophage infiltration are shown in Figure 1a–c.

Localization of JAM-C and ICAM-1

The abundance of JAM-C and ICAM-1 in WT mice kidneys was examined by immunohistochemistry. Sections were subjected to antigen retrieval. Sections were preincubated in a blocking solution (10% goat serum in phosphate-buffered saline or power block, respectively) for 20 min and incubated either overnight at 4°C with monoclonal anti-JAM-C antibody (HM 1057; HyCult Biotechnology, Uden, The Netherlands) or with the anti-mouse ICAM-1 antibody (Santa Cruz Biotechnology Inc., CA) for 1 h at 37°C. Biotinylated goat anti-rat IgG and rabbit anti-goat IgG (Southern Biotechnology Associates, Inc., Birmingham, AL) were used as second antibodies. Sections were incubated for 30 min with ABC reagent (Vectastain, Vector Laboratories, Burlingame, CA). Each section was placed in diaminobenzidine/hydrogen peroxide solution, and counterstained with methylene blue or hemalaun. Representative photomicrographs of JAM-C and ICAM-1 expression are shown in Figure 8a–f.

Detection of apoptosis

As described previously,[49] apoptotic cells were detected by the terminal deoxynucleotidyl transferase-mediated deoxyuridine triphosphate-biotin nick-end labeling (TUNEL) assay (ApopTag Peroxidase In Situ Apoptosis Detection Kit, Intergen, Purchase, NY). Cells were regarded as TUNEL positive if their nuclei were stained brown and displayed typical apoptotic morphology with chromatin condensation. The number of TUNEL-positive cells in each kidney was calculated in a blinded fashion by counting the number of TUNEL-positive tubular cells in 12 sequentially selected fields at $\times 400$ magnification and expressed as the mean number $\pm$ s.e. per 12 high-power fields ($n=6$ in each group). Representative photomicrographs of tubular apoptosis are shown in Figure 1d–f.

Measurement of tubular atrophy

Kidney sections were stained with periodic acid Schiff for assessment of tubular basement membranes, and tubular atrophy was determined as described previously.[50] Atrophic tubules were identified by their thickened and sometimes duplicated basement membranes. The number of atrophic tubules per field at $\times 400$ magnification was counted, and 12 fields/kidney were analyzed. Representative photomicrographs of tubular atrophy are shown in Figure 1g–i.

Morphometric evaluation of the interstitial fibrosis of the renal cortex

Interstitial collagen deposition was measured in Masson trichrome-stained sections as described before.[51] Digital images of the sections were superimposed on a grid and the number of grid points overlapping interstitial blue-staining collagen was recorded for each field. Twelve non-overlapping fields at $\times 400$ magnification were analyzed. Representative photomicrographs of interstitial fibrosis are shown in Figure 1j–l.

Antibodies

Anti-LFA-1 antibody (M17-4), anti-Mac-1 antibody (M-19) and anti-ICAM-1 antibody (M-19) were purchased from Santa Cruz Biotechnology Inc. CA. Goat anti-RAGE antibody was obtained from Merck, Sharpe and Dhome (Harlow, UK). Anti-JAM-C antibody (HM 1057) was purchased from HyCult Biotechnology (Uden, The Netherlands). The anti-mouse JAM-C antibody used for Western blot studies was kindly provided by Dr B Imhof (University of Geneva, Switzerland).

Western immunoblotting

Additional 24 neonatal WT mice underwent UUO surgery or sham operation at the second day of life. Kidneys were harvested 1, 5 and 12 days after obstruction ($n=4$ in each group), homogenized in protein extraction buffer (Triton-X 100 1%, Tris 100 mM, $Na_4P_2O_3$ 100 mM, NaF 100 mM, ethylenediaminetetraacetic acid 10 mM) containing a cocktail of proteinase and phosphatase inhibitors (1 mM Na_3VO_4, 1 mM phenylmethylsulfonyl fluoride, 10 μg/ml leupeptin, 10 μg/ml aprotinin), and centrifuged for 60 min at 20 000 *g*. Fifty micrograms of protein were separated on polyacrylamide gels at 180 V for 45 min and blotted onto nitrocellulose membranes (105 V, 80 min). After blocking for 1 h in Tris-buffered saline with Tween 20 containing 5% nonfat dry milk, blots were incubated with primary antibodies at 4°C overnight. Blots were washed with Tris-buffered saline with Tween 20 and incubated with horseradish peroxidase-conjugated secondary antibody for 1 h at room temperature. Immune complexes were detected using enhanced chemiluminescence (Amersham Pharmacia Biotech, Freiburg, Germany). Blots were exposed to X-ray films (Kodak, Stuttgart, Germany), and protein bands were quantified using densitometry. Each band represents one single mouse kidney.

Immunoprecipitation

For immunoprecipitation, additional eight neonatal WT mice underwent UUO or sham operation within 48 h after birth. Kidneys were harvested 5 days after obstruction ($n = 4$ in each group). The kidney homogenization for immunoprecipitation was performed in 200 μl radioimmunoprecipitation assay-buffer (50 ml phosphate-buffered saline, 500 μl IGEPAL CA-630, 250 mg sodium deoxycholate, 500 μl 10% sodium dodecyl sulfate) containing a cocktail of proteinase and phosphatase inhibitors (1 mM Na_3VO_4, 1 mM phenylmethylsulfonyl fluoride, 10 μg/ml leupeptin, 10 μg/ml aprotinin, 3 mM benzamidine). Kidney samples were further processed by passing through a 20-gauge needle and syringe several times and centrifuged at 16 000 *g* for 10 min. The supernatant was then incubated with 10 μl of the indicated antibodies on a shaker for 2 h at 4°C. Twenty microliters protein A/G agarose beads were added. After overnight incubation, lysates were centrifuged at 1000 *g* for 10 min at 4°C. The pellets were washed, resuspended in electrophoresis buffer, and immunoblotted as described above. Each band represents one single kidney.

Statistical analysis

Data are presented as mean ± s.e. Comparisons between groups were made using one-way analysis of variance followed by the Student–Newman–Keuls test. Comparisons between left and right kidneys were performed using the Student's *t*-test for paired data. Statistical significance was defined as $P < 0.05$.

ACKNOWLEDGMENTS

This research was supported in part by National Institutes of Health DK52612 grant to Dr Robert L Chevalier. Dr Bärbel Lange-Sperandio is supported by a stipend from the German Research Foundation (DFG) La 1257/2-1. This work was in part supported by a grant from the European Foundation for the Study of Diabetes (AB) and by the SFB 405 to PN and TC. We thank Dr Christie Ballantyne, Baylor College Houston, for providing LFA-1- and Mac-1-deficient mice, and Dr Klaus Ley, University of Virginia, for providing murine breeding pairs.

REFERENCES

1. Fivush BA, Jabs K, Neu AM *et al.* Chronic renal insufficiency in children and adolescents: the 1996 annual report of NAPRTCS. North American Pediatric Renal Transplant Cooperative Study. *Pediatr Nephrol* 1998; **12**: 328–337.
2. Chevalier RL. Perinatal obstructive nephropathy. *Semin Perinatol* 2004; **28**: 124–131.
3. Liapis H. Biology of congenital obstructive nephropathy. *Nephron Exp Nephrol* 2003; **93**: e87–e91.
4. Klahr S. Urinary tract obstruction. *Semin Nephrol* 2001; **21**: 133–145.
5. Diamond JR, Kees-Folts D, Ding G *et al.* Macrophages, monocyte chemoattractant peptide-1, and TGF-beta 1 in experimental hydronephrosis. *Am J Physiol* 1994; **266**: F926–F933.
6. Ricardo SD, Levinson ME, DeJoseph MR, Diamond JR. Expression of adhesion molecules in rat renal cortex during experimental hydronephrosis. *Kidney Int* 1996; **50**: 2002–2010.
7. Shappell SB, Mendoza LH, Gurpinar T *et al.* Expression of adhesion molecules in kidney with experimental chronic obstructive uropathy: the pathogenic role of ICAM-1 and VCAM-1. *Nephron* 2000; **85**: 156–166.
8. Ophascharoensuk V, Giachelli CM, Gordon K *et al.* Obstructive uropathy in the mouse: role of osteopontin in interstitial fibrosis and apoptosis. *Kidney Int* 1999; **56**: 571–580.
9. Lange-Sperandio B, Cachat F, Thornhill BA, Chevalier RL. Selectins mediate macrophage infiltration in obstructive nephropathy in newborn mice. *Kidney Int* 2002; **61**: 516–524.
10. Vielhauer V, Anders HJ, Mack M *et al.* Obstructive nephropathy in the mouse: progressive fibrosis correlates with tubulointerstitial chemokine expression and accumulation of CC chemokine receptor 2- and 5-positive leukocytes. *J Am Soc Nephrol* 2001; **12**: 1173–1187.
11. Zhang G, Kim H, Cai X *et al.* Urokinase receptor modulates cellular and angiogenic responses in obstructive nephropathy. *J Am Soc Nephrol* 2003; **14**: 1234–1253.
12. Ricardo SD, Diamond JR. The role of macrophages and reactive oxygen species in experimental hydronephrosis. *Semin Nephrol* 1998; **18**: 612–621.
13. Hirschberg R, Wang S. Proteinuria and growth factors in the development of tubulointerstitial injury and scarring in kidney disease. *Curr Opin Nephrol Hypertens* 2005; **14**: 43–52.
14. Lange-Sperandio B, Fulda S, Vandewalle A, Chevalier RL. Macrophages induce apoptosis in proximal tubule cells. *Pediatr Nephrol* 2003; **18**: 335–341.
15. Chow FY, Nikolic-Paterson DJ, Atkins RC, Tesch GH. Macrophages in streptozotocin-induced diabetic nephropathy: potential role in renal fibrosis. *Nephrol Dial Transplant* 2004; **19**: 2987–2996.
16. Diamond JR. Macrophages and progressive renal disease in experimental hydronephrosis. *Am J Kidney Dis* 1995; **26**: 133–140.
17. Shappell SB, Gurpinar T, Lechago J *et al.* Chronic obstructive uropathy in severe combined immunodeficient (SCID) mice: lymphocyte infiltration is not required for progressive tubulointerstitial injury. *J Am Soc Nephrol* 1998; **9**: 1008–1017.
18. Le Meur Y, Tesch GH, Hill PA *et al.* Macrophage accumulation at a site of renal inflammation is dependent on the M-CSF/c-fms pathway. *J Leukoc Biol* 2002; **72**: 530–537.
19. Takeda A, Fukuzaki A, Kaneto H *et al.* Role of leukocyte adhesion molecules in monocyte/macrophage infiltration in weanling rats with unilateral ureteral obstruction. *Int J Urol* 2000; **7**: 415–420.
20. Kriegsman J, Muller H, Sommer M *et al.* Expression of LFA-1 (CD11a/CD18) and ICAM-1 (CD54) in an animal model of renal interstitial fibrosis induced by unilateral ureteral obstruction. *Exp Toxicol Pathol* 2000; **52**: 185–191.
21. Butcher EC. Leukocyte–endothelial cell recognition – three (or more) steps to specificity and diversity. *Cell* 1991; **67**: 1033–1036.
22. Dunne JL, Collins RG, Beaudet AL *et al.* Mac-1, but not LFA-1, uses intercellular adhesion molecule-1 to mediate slow leukocyte rolling in TNF-alpha-induced inflammation. *J Immunol* 2003; **171**: 6105–6111.
23. Henderson RB, Lim LH, Tessier PA *et al.* The use of lymphocyte function-associated antigen (LFA)-1-deficient mice to determine the role of LFA-1, Mac-1, and alpha4 integrin in the inflammatory response of neutrophils. *J Exp Med* 2001; **194**: 219–226.
24. Yamagishi H, Yokoo T, Imasawa T *et al.* Genetically modified bone marrow-derived vehicle cells site specifically deliver an anti-inflammatory cytokine to inflamed interstitium of obstructive nephropathy. *J Immunol* 2001; **166**: 609–616.
25. Cheng QL, Chen XM, Li F *et al.* Effects of ICAM-1 antisense oligonucleotide on the tubulointerstitium in mice with unilateral ureteral obstruction. *Kidney Int* 2000; **57**: 183–190.
26. Liliensiek B, Weigand MA, Bierhaus A *et al.* Receptor for advanced glycation end products (RAGE) regulates sepsis but not the adaptive immune response. *J Clin Invest* 2004; **113**: 1641–1650.
27. Chavakis T, Bierhaus A, Al Fakhri N *et al.* The pattern recognition receptor (RAGE) is a counterreceptor for leukocyte integrins: a novel pathway for inflammatory cell recruitment. *J Exp Med* 2003; **198**: 1507–1515.
28. Schmidt AM, Yan SD, Yan SF, Stern DM. The multiligand receptor RAGE as a progression factor amplifying immune and inflammatory responses. *J Clin Invest* 2001; **108**: 949–955.
29. Abel M, Ritthaler U, Zhang Y *et al.* Expression of receptors for advanced glycosylated end-products in renal disease. *Nephrol Dial Transplant* 1995; **10**: 1662–1667.
30. Wendt TM, Tanji N, Guo J *et al.* RAGE drives the development of glomerulosclerosis and implicates podocyte activation in the pathogenesis of diabetic nephropathy. *Am J Pathol* 2003; **162**: 1123–1137.
31. Bazzoni G. The JAM family of junctional adhesion molecules. *Curr Opin Cell Biol* 2003; **15**: 525–530.
32. Ebnet K, Suzuki A, Ohno S, Vestweber D. Junctional adhesion molecules (JAMs): more molecules with dual functions? *J Cell Sci* 2004; **117**: 19–29.
33. Keiper T, Santoso S, Nawroth PP *et al.* The role of junctional adhesion molecules in cell–cell interactions. *Histol Histopathol* 2005; **20**: 197–203.
34. Santoso S, Sachs UJ, Kroll H *et al.* The junctional adhesion molecule 3 (JAM-3) on human platelets is a counterreceptor for the leukocyte integrin Mac-1. *J Exp Med* 2002; **196**: 679–691.
35. Johnson-Leger CA, Aurrand-Lions M, Beltraminelli N *et al.* Junctional adhesion molecule-2 (JAM-2) promotes lymphocyte transendothelial migration. *Blood* 2002; **100**: 2479–2486.

36. Zen K, Babbin BA, Liu Y *et al.* JAM-C is a component of desmosomes and a ligand for CD11b/CD18-mediated neutrophil transepithelial migration. *Mol Biol Cell* 2004; **15**: 3926–3937.
37. Pluskota E, Soloviev DA, Plow EF. Convergence of the adhesive and fibrinolytic systems: recognition of urokinase by integrin alpha Mbeta 2 as well as by the urokinase receptor regulates cell adhesion and migration. *Blood* 2003; **101**: 1582–1590.
38. Pluskota E, Soloviev DA, Bdeir K *et al.* Integrin alphaMbeta2 orchestrates and accelerates plasminogen activation and fibrinolysis by neutrophils. *J Biol Chem* 2004; **279**: 18063–18072.
39. Simon DI, Wei Y, Zhang L *et al.* Identification of a urokinase receptor-integrin interaction site. Promiscuous regulator of integrin function. *J Biol Chem* 2000; **275**: 10228–10234.
40. Matsui H, Suzuki M, Tsukuda R *et al.* Expression of ICAM-1 on glomeruli is associated with progression of diabetic nephropathy in a genetically obese diabetic rat, Wistar fatty. *Diabetes Res Clin Pract* 1996; **32**: 1–9.
41. Tang T, Rosenkranz A, Assmann KJ *et al.* A role for Mac-1 (CDIIb/CD18) in immune complex-stimulated neutrophil function *in vivo*: Mac-1 deficiency abrogates sustained Fcgamma receptor-dependent neutrophil adhesion and complement-dependent proteinuria in acute glomerulonephritis. *J Exp Med* 1997; **186**: 1853–1863.
42. Soma J, Saito T, Ootaka T *et al.* Intercellular adhesion molecule-1, intercellular adhesion molecule-3, and leukocyte integrins in leukocyte accumulation in membranoproliferative glomerulonephritis type I. *Am J Kidney Dis* 1996; **28**: 685–694.
43. Brett J, Schmidt AM, Yan SD *et al.* Survey of the distribution of a newly characterized receptor for advanced glycation end products in tissues. *Am J Pathol* 1993; **143**: 1699–1712.
44. Chavakis T, Bierhaus A, Nawroth PP. RAGE (receptor for advanced glycation end products): a central player in the inflammatory response. *Microbes Infect* 2004; **6**: 1219–1225.
45. Vestweber D. Regulation of endothelial cell contacts during leukocyte extravasation. *Curr Opin Cell Biol* 2002; **14**: 587–593.
46. Chavakis T, Keiper T, Matz-Westphal R *et al.* The junctional adhesion molecule-C promotes neutrophil transendothelial migration *in vitro* and *in vivo*. *J Biol Chem* 2004; **279**: 55602–55608.
47. Ding ZM, Babensee JE, Simon SI *et al.* Relative contribution of LFA-1 and Mac-1 to neutrophil adhesion and migration. *J Immunol* 1999; **163**: 5029–5038.
48. Lu H, Smith CW, Perrard J *et al.* LFA-1 is sufficient in mediating neutrophil emigration in Mac-1-deficient mice. *J Clin Invest* 1997; **99**: 1340–1350.
49. Cachat F, Lange-Sperandio B, Chang AY *et al.* Ureteral obstruction in neonatal mice elicits segment-specific tubular cell responses leading to nephron loss. *Kidney Int* 2003; **63**: 564–575.
50. Chevalier RL, Thornhill BA, Chang AY *et al.* Recovery from release of ureteral obstruction in the rat: relationship to nephrogenesis. *Kidney Int* 2002; **61**: 2033–2043.
51. Fern RJ, Yesko CM, Thornhill BA *et al.* Reduced angiotensinogen expression attenuates renal interstitial fibrosis in obstructive nephropathy in mice. *J Clin Invest* 1999; **103**: 39–46.